SEAGC

by Muhamad Yusa

Submission date: 03-Apr-2021 10:27AM (UTC+0700)
Submission ID: 1549414560
File name: 18SEAGC-Paper-Final.pdf (432.25K)
Word count: 2068
Character count: 11204

18th Southeast Asian Geotechnical & Inaugural AGSSEA Conference
29 - 31 May 2013, Singapore
Leung, Goh & Shen (eds)

MEASUREMENT AND CHANGE IN MICROSTRUCTURE OF LOOSE SILTY SAND DUE TO AGING

MUHAMAD YUSA
Civil and Natural Resources Engineering, University of Canterbury, New Zealand,
myu20@uclive.ac.nz

ELISABETH T. BOWMAN
Civil and Natural Resources Engineering, University of Canterbury, New Zealand,
elisabeth.bowman@canterbury.ac.nz

Recently, imaging technology has been used in geotechnical engineering to enhance our understanding of microscopic characteristics and micro-mechanical behaviour of sands. In this study, silty sand samples loaded uniaxially under K_0 condition for various aging times were preserved using low viscosity epoxy resin. High quality images were captured by scanning electron microscope utilizing a backscattered electron detector giving excellent contrast between the grains and voids. This paper discusses challenges in image analysis and initial results that show that statistically, during aging under load, the larger particles rotate with time.

INTRODUCTION

It is well known that macro-mechanical behavior of sand is highly dependent on its particle arrangement and its associated pore spaces, thus its microstructure. In the last fifty years, field evidence has revealed that over years, months and days time has a significant effect on the mechanical behaviour of sand. Examples include increases in cone penetration resistance [1, 2] after ground improvement such as via vibro-compaction and explosive blasting. This phenomenon is usually referred to as *sand aging*. Another beneficial effect of sand aging is increase in liquefaction resistance [3, 4].

MECHANISM OF AGING

There has been no consensus yet about mechanisms behind sand aging. In general, there are two main suggested mechanisms, chemical and mechanical. Some researchers [5, 6] have attributed the aging to cementation at the contact points between grains due to the formation of silica acid gel films on particle surfaces and the precipitation of silica or other materials from solution or suspension. Other researchers [7, 8] have attributed aging to creep processes, where particle rearrangement results in a greater interlocking of particles and consequently, greater frictional resistance. Mechanical aging probably occurs over a period of weeks to months while, for longer durations (e.g., years), chemical mechanisms may play a more significant role. This study is an attempt to enhance our understanding about sand aging by investigating microscopic changes that occur during aging. This paper focuses on the methods used to obtain good quality data and initial results in terms of changes in soil fabric over time.

EXPERIMENTAL PROGRAM

Material

The material used in this research program is silty sand. Silty sand was chosen considering that majority of previous laboratory research on sand aging has been performed on clean sand while sands containing fines are far more common in nature. Silty sand was reconstituted in the laboratory by mixing sand and fine fractions (<75um). The sand fraction was collected from a site that liquefied during the Darfield Earthquake, Christchurch, New Zealand in 2010. Sand particle diameters range from 75μm to 300μm. The fine fraction is non-plastic silica flour with diameter range from 32μm to 75μm. The percentage of fine fraction used in this study is 15%, a typical fines content of Christchurch's sand. The specific gravities Gs of the sand and silt ranged from 2.64 to 2.65. Maximum and minimum void ratios of the silty sand are 0.973 and 0.565 respectively. Figure 1 shows the particle size distribution of the combined soils.

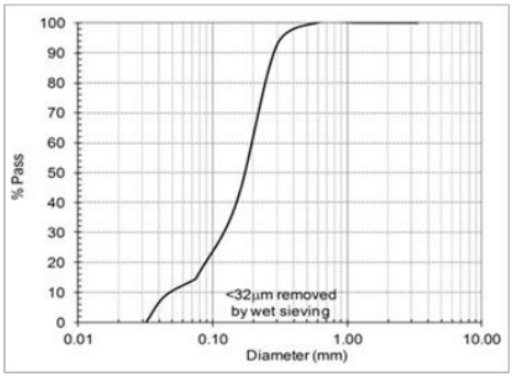

Figure 1. Combined particle size distribution.

Sample reconstitution and preservation

Specimens were prepared in the impregnation cylinder by moist tamping method [9]. While moist tamping does not replicate natural deposition, segregation of fines does not occur as may happen with pluviation and other preparation methods. A low viscosity and shrinkage epoxy curing agent, EPO-THIN, by Buehler Inc. was impregnated into the specimen. The epoxy mixture ratio (by weight) of resin, hardener and acetone was 100:39:12. Prior to impregnation, the moist soil specimen needed to be dried because epoxy resins do not cure well in a moist environment.

An apparatus to preserve the soil fabric using epoxy resin adapted from Masad [10] was used with a modification to enable the fitting to be used many times. The setup for impregnation of the specimen is shown by Figure 2. The soil sample prepared to a relative density of 40% was loaded under zero lateral strain (K_0 condition). Load was chosen as 30 kPa to simulate loose silty sand that is prone to liquefaction at shallow depth. Muszynki [11] found significant changes in pore size distribution of silty soil that was left in secondary compression for one hour and five days, respectively, thus similar aging times were used in this study. The epoxy resin was injected into

the base pedestal of the impregnation chamber using a low pressure of 15-25kPa to minimize disturbance and presence of air bubbles. Dial gauges were used to observe the volume of epoxy injected and to monitor displacement of the specimen.

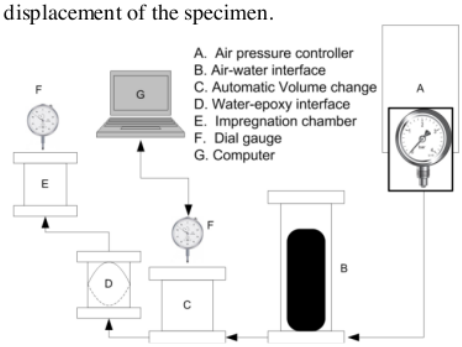

Figure 2. Setup for soil preservation

Coupon Preparation

Once the epoxy impregnated specimen was fully cured (about two weeks), it was removed from the impregnation chamber. The sample then cut and polished with successively finer abrasive discs and finally alumina powder .

Capturing Image

Images from the polished coupons were captured using a high resolution field emission Scanning Electron Microscope (SEM). This was done after several attempts using optical microscopy did not give enough contrast between the grains and epoxy filled voids. Two methods of capturing images using SEM were performed i.e. conventional secondary electron detector (SED) and back scattered detector (BSD). SED is based on surface specimen topography. BSD on the other hand is based on atomic weight of the material. High atomic number material will appear brighter than the lower one [12]. Secondary electron produces images that contain less detail (e.g. edge grains boundary) compared to back scattered images (especially when the surface specimen had been polished flat) as exemplified in Figure 3a and Figure 3b. Thus BSD was used in this study.

Image Processing

Captured images were then processed and analysed using image analysis software *ImageJ* and *Image Pro Plus 7.0*. Enhancement of the image was done by *ImageJ*. Steps involved in this process include contrast expansion, correction for noise and thresholding. The resulting image is displayed as a binary image using black and white colours to distinguish foreground and background regions, as shown in Figure 3(c). Subsequent steps were filling the grain holes and watershed splitting to separate the grains.

Microstructures Measurements

Generally there are two common measures to quantify the microstructure i.e. particle orientation and void ratio. However due to space constraint this paper will only describes measurement and change in particle orientation.

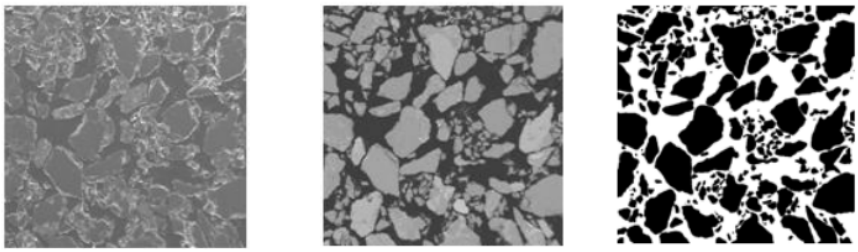

(a) (b) (c)

Figure 3 Typical image (a) SED (b) BSD; (c) after image processing

Particle orientation is usually defined by the angle of the apparent long axis. This measure can be either presented by a histogram or a rose diagram. The authors believe that rose diagrams give a more intuitive sense of the particle orientation distribution thus rose diagrams are used here. Statistical parameters were then determined to summarize the distribution of particle orientation using Fisher distribution analysis [13].The Fisher distribution function $P_{dA}(\alpha)$ gives the normalized probability of finding a unit vector direction within an angular area dA, at angle of α from true mean direction(at which α=0). The Fisher distribution is defined as:

$$P_{dA}(\alpha) = \frac{\kappa}{2\pi \sinh(\kappa)} \exp[\kappa . \cos(\alpha)] \sin(\alpha) \quad \text{Eq.1}$$

Where α is the angle between the unit vector and the true direction and κ is a precision parameter and is a measure of the concentration of the distribution about the true mean direction.

The influence of different scales of structure on the behaviour of soil is unknown. A soil with a relatively large number of fine particles (silt) may have different scales of interest. The results of rose diagrams in which all fines are included, for example, will be controlled by the fine particles although the large particles may form the major force columns and govern the soil's mechanical behaviour. To avoid bias related to particle size, a weighted value for the orientation of each particle is displayed here. Thus the resultant vector length (R) and mean angle (α_m) can be determined as follows:

$$R^2 = \sqrt{\left\{\sum_{i=1}^{N} [l_i . \sin(2\alpha]\right\}^2 + \left\{\sum_{i=1}^{N} [l_i . \cos(2\alpha]\right\}^2} \quad \text{Eq.2}$$

$$\alpha_m = \frac{1}{2} tan^{-1}\left(\left\{\sum_{i=1}^{N}[l_i \sin(2\alpha_i)]\right\} / \left\{\sum_{i=1}^{N}[l_i \cos(2\alpha_i)]\right\}\right) \quad \text{Eq.3}$$

Where l_i is the length of long axes of the particle and N is the number of measurements. The precision parameter κ or degree of cluster can be estimated from

$$\kappa = \frac{N-1}{N-R} \quad \text{Eq.4}$$

Finally, a parameter called the mean of dispersion (R/N) is also used in this study.

RESULTS

Approximately 5500 particles (detailed number is in Table 1) from 20 images per test were measured for distribution of particle orientation. Figure 4a shows distribution of particle orientation for one hour aging time. This test provided a 'baseline' of initial fabric, which others test (one week aging time in this study), could then be compared. The results indicate that the distribution of particle orientations prepared by moist tamping are generally random, as found by previous researchers. From the Fisher analysis, Table 1, the mean direction is 15.5^0 and degree of clustering, κ , is 2.15.

Figure 4b shows the result of the same loading which was applied for one week before preserved by epoxy resin. This test was performed to see whether any changes, if any, could be observed in the soil structure over time under load, compare to 'baseline' test. The rose diagram shows slightly changes in number of particles oriented at various degrees. The mean direction change to -34.7^0 compared to 15.5^0 in baseline test, indicating aging cause some particles to rotate. The degree of clustering increases approximately 28%. Likewise, the dispersion increases 10.28%, indicating that during aging of loose silty sand orientation of the particles more spread.

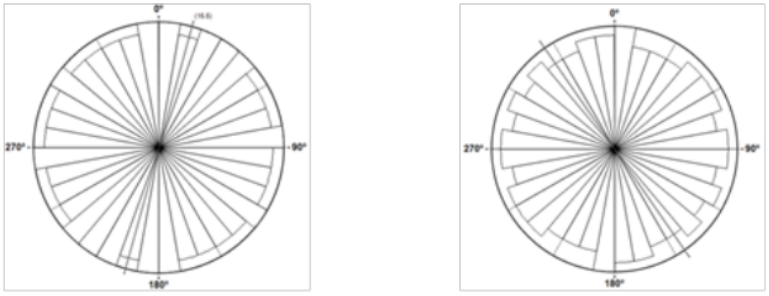

(a) 1 hour aging (b) 1 week aging

Figure 4. Rose diagram for 1 hour and 1 week of aging

Table 1. Fisher distribution analysis results

Aging time	No. particles	Dispersion, R/N %	Mean Direction, α_m degree	Cluster, κ
1 hour	5244	53.54	15.5	2.15
1 week	5873	63.82	-34.7	2.76

CONCLUSION

There has been no consensus about mechanism behind sand aging. This study is attempting to enhance our understanding about sand aging mechanisms. A SEM via electron backscattered detector was used to investigate microscopic changes that occur during aging. The tendency is found that although aging only causes a slight change in overall global density, over time particles rotate. Additional statistical analysis on the spatial distribution of distance between particles will be given in future papers.

REFERENCES

[1] Schmertmann, J. H., Baker, W., Gupta, R., & Kessler, K., "CPT/DMT QC of Ground Modification at a Power Plant", *Use of In situ Tests in Geotechnical Engineering*, ASTM STP No. 6, (1986), pp 985-1001.

[2] Debats, J.-M., & Sims, M., "Vibroflotation in Reclamations in Hong Kong" , *Proceedings of the ICE - Ground Improvement,* Vol.1 (1997), pp. 127-145

[3] Seed, H. B., "Soil liquefaction and cyclic mobility evaluation for level ground during earthquakes ", *Journal of the Geotechnical Engineering Division,* Vol. 105 (GT2), (1979), pp. 201-255.

[4] Troncoso, J., Ishihara, K., & Verdugo, R., "Aging effect on cyclic shear strength of tailing material". *Proc. IX World Conference on Earthquake Engineering*, Tokyo-Kyoto. (1988).

[5] Mitchell, J. K., & Solymar, Z. V., "Time-Dependent Strength Gain in Freshly Deposited or Densified Sand", *Journal of Geotechnical Engineering,* Vol. 110, No. 11, (1984), pp.1559-1576.

[6] Sheldon, H. A., & Wheeler, J., "Influence of Pore Fluid Chemistry on the state ofStress in Sedimentary Basins", *Geological Society of America,* Vol. 31., No. 1, (2003), pp.59-62.

[7] Schmertmann, J. H. (1991). "The Mechanical Aging of Soils", *Journal of Geotechnical Engineering,* Vol. 117, No. 9, pp. 1288-1330.

[8] Bowman, E. T., & Soga, K.. "Creep, aging and microstructural change in dense granular materials", *Soils and Foundations,* Vol. 43, No. 4, (2003), pp. 107-117.

[9] Ladd, R., " Preparing Test Specimens Using Undercompaction", *ASTM Geotechnical Testing Journal,* Vol. 1, No. 1, (1978), pp.16-23.

[10] Masad, E., *Permeability simulation of reconstructed anisotropic soil medium,* Phd Theses, Washington State University, (1998).

[11] Muszynski, M.R., *Void ratio distribution of Normally consolidated corase-grain magnetic tailings as a function of aging time*, M.S. Thesis, Michigan Technological University, (2000).
[12] Lloyd, G., "Atomic number and chrystallographic contrast images with the SEM: a review of backscattered electron techniques", *Mineralogical Magazine, 51,* (1987), pp. 3-19.
[13] Fisher, RA., "Dispersion on a sphere", *Proc. Roy. Soc. London Ser. A.*, Vol. 217, (1953), pp 295–305.

SEAGC

ORIGINALITY REPORT

14%	14%	5%	%
SIMILARITY INDEX	INTERNET SOURCES	PUBLICATIONS	STUDENT PAPERS

PRIMARY SOURCES

1	followscience.com Internet Source	3%
2	geo.shef.ac.uk Internet Source	3%
3	magician.ucsd.edu Internet Source	2%
4	discovery.ucl.ac.uk Internet Source	2%
5	tpdsci.com Internet Source	1%
6	Jianting Zhu. "Impact of scaling break and fracture orientation on effective permeability of fractal fracture network", SN Applied Sciences, 2018 Publication	1%
7	www.ic2e.org Internet Source	1%
8	link.springer.com Internet Source	1%

Exclude quotes	On	Exclude matches	< 1%
Exclude bibliography	On		